UNIVERSIDADE DE SÃO PAULO

INSTITUTO DE FÍSICA
CAIXA POSTAL 20516
01498 - SÃO PAULO - SP
BRASIL

PUBLICAÇÕES

IFUSP/P-703

OPTICAL ABSORPTION STUDY OF RADIATION AND THERMAL EFFECTS IN BRAZILIAN SAMPLES OF SPODUMENE

Sadao Isotani, Américo Tsuneo Fujii, Rodolfo Antonini and Wagner Wilson Furtado

Instituto de Física, Universidade de São Paulo

Março/1988

OPTICAL ABSORPTION STUDY OF RADIATION AND THERMAL EFFECTS IN BRAZILIAN SAMPLES OF SPODUMENE

Sadao Isotani, Américo Tsuneo Fujii, Rodolfo Antonini and Wagner Wilson Furtado

Instituto de Física, Universidade de São Paulo
C.P. 20516, 01498 São Paulo, SP, Brazil

Key words: Spodumene, Optical Absorption, Radiation Effects, Thermal Blanching.

ABSTRACT

Irradiation induced 10,500 and 15,600 cm^{-1} optical absorption bands in Mn and Fe rich samples of spodumene was shown to be associated to a single center through irradiation growth and thermal bleaching analysis. Polarized optical absorption study showed two bands around ~ 13,000 and ~ 21,000 cm^{-1}, which we assigned tentatively to interstitial Fe^{2+} ion and the single center. Discussions lend us to assign the 6,100 and 9,000 cm^{-1} doublet of green and yellow Fe and Mn rich samples of spodumene to Fe^{2+} ion at $A\ell^{3+}$ site stabilized by a +2e cation at Li^{+} site; the 16,000 cm^{-1} in these samples to Fe^{2+}-Fe^{3+} charge transfer between Fe^{2+} and Fe^{3+} ions at neighbour $A\ell^{3+}$ sites and stabilized by a +2e cation at Li^{+} site; the single center to Mn^{3+} at $A\ell^{3+}$ site, which arises by the trapping of an electron by Mn^{4+} ion stabilized by a +2e cation substitution at a neighbour $A\ell^{3+}$ site; and the 18,600 cm^{-1} band of lilac Mn rich spodumene to Mn^{3+} at $A\ell^{3+}$ site, which arises by the trapping of an electron by Mn^{4+} ion stabilized by the vacancy of a neighbour Li^{+} ion.

I. INTRODUCTION

We report here a new detailed analysis of the previous reported optical absorption (OA) spectra of five varieties of brazilian spodumene (Fujii, 1981).

The spodumene is a silicate belonging to the inosilicate class of formula $LiAlSi_2O_6$ (Dana and Hurlbut, 1978, p. 470-480). The unit cell contains four chemical units, with the parameters a = 9.50 Å, b = 8.30 Å and c = 5.24 Å. It belongs to spatial group C2/c with perfect cleavage plane (010) forming angles of 87° and 93° (Deer et al., 1966, p. 92-98). There are four equivalent sites for Li^+ and Al^{3+} with an axis of order 2 parallel to the b-axis.

It is very common to find ions of Na^+ substituting for Li^+. Other impurities usually found in spodumene are Fe, Mn, Cr and V. A relationship between the color and the presence of impurities was observed. This relationship depends on the site occupied by these impurities in the crystal lattice, on their valence state, coordination and concentration.

Spodumene is a source for the production of Li salts. The transparent varieties of beautiful coloration

are gemstones. These are known as kunzite (lilac), hiddenite (green) and spodumene (colorless or yellow). Heat treatment as well as irradiation with γ-rays, X-rays, electrons and ultraviolet light causes changes in color. Extensive studies have already been done on spodumene (Claffy, 1953; Manoogian et al.,1965; Holuj, 1968; Holuj and Manoogian, 1968; Gait and Michoulier, 1973; Leckebush et al., 1974; Schmitz and Lehman, 1975; Hassan and Labib, 1978; Ito, 1980).

The kunzite, lilac variety of spodumene has an absoprtion band around 18,600 cm^{-1} and an ultraviolet band-edge around 29,000 cm^{-1}. When irradiated with ionizing radiation, a strong band at around 15,600 cm^{-1} covers the 18,600 cm^{-1} band and the ultraviolet band-edge shifts to 24,000 cm^{-1}. In this case the kunzite turns green. When heated to temperatures above 120°C the green color disappears in a few hours returning to the initial color. Heating above 300°C bleaches the lilac color, which can be restored by irradiation followed by heating at temperatures between 120°C and 300°C. Ito (1980) showed through thermal and irradiation dose kinetics of the absorption bands, that the 15,600 cm^{-1} (green band) and 18,600 cm^{-1} (lilac band) bands are independent.

The Mn^{2+} EPR spectra of natural kunzite crystals showed that Mn^{2+} ion is substitutional to the Al^{3+} ion and are changed on heating, passing from two main groups, Mn^{2+}(I) and Mn^{2+}(II-V) to Mn^{2+}(I) (Holuj and Manoogian, 1968). However, after this treatment, neither irradiation nor heating changes the EPR spectra of Mn^{2+}(I) ion (Ito, 1980). Polarized optical absorption spectra of green and lilac bands was shown to be allowed for octahedral symmetry (Ito, 1980). In this way 15,600 cm^{-1} and 18,600 cm^{-1} bands were assigned to Mn^{3+} in two different sites, say, Mn^{3+}(a) and Mn^{3+}(b), respectively.

The five varieties of spodumene studied by Fujii (1981) are lilac, colorless I, colorless II, green and yellow samples, with Mn, Fe and Cr concentrations as given in table I. The lilac, colorless I and colorless II

Insert Table I

samples when irradiated turns intensely green, but on heating at 200°C the lilac and colorless I turns lilac and the colorless II turns colorless. The OA spectra of these samples show several

bands. In table II we give the band positions and the previously and the present suggested assignment.

Insert Table II

The two bands observed in colorless I, green and yellow samples at ~6,100 and ~9,000 cm^{-1} can be assigned to the d-d electronic transition of Fe^{2+} in distorted octahedral site (Burns, 1970, p. 78). The ratio between the magnitudes of the Fe^{2+} electronic (9,000 cm^{-1}) and Fe^{2+}-Fe^{3+} charge transfer (16,000 cm^{-1}) bands in the green sample is about 0.5 and in the yellow sample is 4.5 . This observation suggests that enough amounts of Fe^{3+} are near Fe^{2+} in green, yellow, and colorless I samples, being bigger in the green spodumene and smaller in colorless I spodumene. In lilac and colorless II samples the absence of the Fe^{2+}-Fe^{3+} charge transfer band suggests that there is no Fe^{3+} available to form Fe^{2+}-Fe^{3+} coupling.

The band at 18,600 cm^{-1} was shown to be independent of the 15,600 cm^{-1} through the analysis of the OA spectra of heated lilac sample. This observation was reinforced by similar studies in colorless I sample

(Fujii, 1981). Also liquid N_2 temperature OA spectra of lilac sample show that the two bands are independent (Fujii, 1981). Alhtough Ito (1980) have assigned the band at 18,600 cm^{-1} to Mn^{3+}(b) ion, we propose in the present report a different assignment.

Irradiation and heating does not change the color of yellow and green samples (Fujii, 1981). The OA bands at 6,100 cm^{-1} and 9,000 cm^{-1} in these samples, and also in lilac sample, are not changed by irradiation and heating. So, we conclude that these treatments does not change the concentration of Fe^{2+} and Fe^{3+}.

The lilac, colorless I and colorless II samples turns intensely green under irradiation. The OA spectrum show the appearing of a 15,600 cm^{-1} band for $\underline{E} \perp \underline{c}$-axis, and 10,500 cm^{-1} and 15,600 cm^{-1} bands for $\underline{E} // \underline{c}$-axis. The line shape of these bands in the colorless II sample are not deformed by the 18,600 cm^{-1} band. So, we give our attention in the present report to the analysis of the OA spectra of the colorless sample.

II. EXPERIMENTAL

The sample of colorless II spodumene were obtained in Minas Gerais, Brazil, and was studied previously by Fujii (1981). They showed cleavage (110) planes and 93° angles between the ($\bar{1}$10) planes. This morphology together with the known growth direction along the $\underline{c}$-axis allowed us to identify all crystallographic axis.

The samples were cut in two forms: (i) parallelopiped with two faces perpendicular to the $\underline{c}$-axis and two faces parallel to the cleavage plane with ~5 × 5 × 10 mm; (ii) faceted circular with two parallel faces perpendicular to the $\underline{c}$-axis.

A Carl-Zeiss DMR 21 spectrophotometer was used for the optical absorption (OA) measurements. Polarized light measurements were done with Type II polaroid.

The thermal treatments were done in air. The stability of the furnace with useful volume 10 × 12 × 15 cm was improved to 1°C by filling with brick materials and two metallic plates. The temperature was measured using a chromel-alumel thermocouple, with one junction at 0°C with ECB X-T recorder and a Keithey 160B digital multimeter.

All the samples to be treated were put between previously heated metallic plates. With this set we obtained thermal equilibrium in the samples in about 40 seconds, and the error in the treatment time was estimated to be about 20 seconds (Fujii and Isotani, 1982).

The samples were γ-irradiated using a ^{60}Co-source (~ 400.000 Ci) from EMBRARAD S.A.. The dose was controlled by means of three processes: Ceric-Cerous dosimetric system, AECL Red Acryllic dosimetric system and UKAEA Red Perspex dosimeter.

III. RESULTS

a) Irradiation

Irradiation of colorless II spodumene produce two bands at 10,500 cm^{-1} and 15,600 cm^{-1}, as shown in figure 1.

Insert Figure 1

The irradiation growth of the 15,600 cm^{-1} band for $\underline{E}$ // $\underline{c}$-axis is shown in figure 2. The solid line

Insert Figure 2

was fit using the Levy's model (1974) for two exponential, giving:

$$A = 0.613(1 - e^{-0.0386D}) + 0.160(1 - e^{-0.8109D}) \quad (1)$$

where D is given in MGy and A is the absorbance. This result indicates that the process of radiation growth of the 15,600 cm^{-1} band is complex.

The band at around 10,500 cm^{-1} in the colorless II sample is a complex band. In this way, we analysed the band-shape of the 10,500 cm^{-1} and 15,600 cm^{-1} bands, assuming that they are formed by a sum of gaussian lines. The analysis showed that the 10,500 cm^{-1} band is composed by at least two gaussian lines and the 15,600 cm^{-1}, probably, by one gaussian line. The general formula used here is:

$$A(\nu) = \sum_{i=1}^{3} A_{oi} \exp\left[-\sigma_i (\nu - \nu_{oi})^2\right] \quad , \quad (2)$$

where ν is given in cm^{-1}, A_{oi}, σ_i and ν_{oi} are constants

(i = 1, 2 for 10,500 cm^{-1} band and i = 3 for 15,600 cm^{-1} band).

The fit were done using the method of linearization of gaussians (Bevington, 1969, p. 204). The results of the fit are good as shown in figure 3 ($\underline{k}//\underline{c}$-axis) and 4 ($\underline{k} \perp \underline{c}$ and (110)-axis). The fit parameters

Insert Figures 3 and 4

are shown in table III. The errors evaluated by comparing

Insert Table III

experimental data with the evaluated curves, but does not included experimental errors. So, differences like observed for σ in $\underline{k}//\underline{c}$-axis and $\underline{k} \perp \underline{c}$- and (110)-axis. Spectra at around 15,600 cm^{-1} are not significative. This observation reinforces the probability that this band is composed by a single gaussian line. On the other hand the differences observed for σ in $\underline{k}//\underline{c}$-axis and $\underline{k} \perp \underline{c}$- and (110)-axis spectra of 10,500 cm^{-1} are significative, meaning that this band is a complex band.

In figure 5, we show the change of the spectra

Insert Figure 5

with the direction of $\underline{k}$ ($\underline{k} \perp$ (110)-axis) along the plane perpendicular to the (110)-axis. We see that the line at around 10,500 cm^{-1} is strongly dependent of the $\underline{k}$ direction, while the 15,600 cm^{-1} show weaker dependence. We see also a shoulder at around 21,000 cm^{-1}.

In figure 6 we show the polarized spectra

Insert Figure 6

for $\underline{k}//\underline{c}$-axis. A new weak line appears between 30° and 60° from $\underline{E} \perp$ (110)-axis at around 22,000 cm^{-1} and a very weak line for 60° at around 12,500 cm^{-1}.

In figure 7, we show the polarized spectra

Insert Figure 7

for $\underline{k}//$(110)-axis. We see a very weak line at around 13,000 cm^{-1} for 150° from the $\underline{c}$-axis, and another weak line at around 20,000 cm^{-1} (broad band maximum varying from 19,500 cm^{-1} to 21,000 cm^{-1} with polarization) for 60° from the $\underline{c}$-axis.

We assign, tentatively, the line around 12,500 ~ 13,000 cm^{-1} to Fe^{2+} ion by analogy to the bands assigned to this ion in several minerals (White and Keester, 1966; Blak et al., 1983). The precursor of this is, probably, an interstitial Fe^{3+} ion reduced into Fe^{3+} by irradiation. The 20,000 ~ 22,000 cm^{-1} band polarization is different from that shown by the band assigned to Fe^{2+} ion. In this region Fe^{2+} and Fe^{3+} ions are not expected to show absorption transitions. On the other hand, Ito (1980) predicted a line at about 21,500 cm^{-1} for Mn^{3+}(a) through crystal field calculation. So, we assign tentatively, the 20,000 ~ 22,000 cm^{-1} band to electronic transition of Mn^{3+}(a) ion.

b) Heating

Irradiation induces green color in colorless II sample. The color is due to the appearing of two bands at 10,500 cm^{-1} and 15,600 cm^{-1}, and a band-edge at the blue region of the spectrum. These bands bleached on heating at 200°C, and the sample turns colorless again.

In figure 8 we show the decay of the 15,600 cm^{-1} band in colorless II sample. The solid line were

Insert Figure 8

obtained from the n-th order single center kinetic model (Takeuchi et al., 1975):

$$\frac{d}{dt} A(t) = s_0 \exp(-\Delta E/kT) A(t)^n \quad , \qquad (3)$$

where ΔE is the activation energy, T is the absolute temperature, k is the Boltzmann constant and t is given in seconds. Assuming that the order n of the kinetics does not change with temperature, the solution of the above kinetic differential equation is:

$$A(t) = A_0(1 + at)^b \quad , \qquad (4)$$

where

$$a = (n-1)\, s_0 \exp(-\Delta E/kT)/A_0$$

$$b = 1/(1-n) \; .$$

In table IV we show the values determined for the para-

Insert Table IV

meters a, b and n. As n changes with temperature, it means that the order of the kinetics changes with temperature, in contradiction with the assumed assumption to solve the kinetic differential equation.

The fit with Levy's model (1974) with three single centers is given by:

$$A(t) = \sum_{i=1}^{3} A_i^0 \exp(-b_i t) \quad , \qquad (5)$$

where A_i^0 and b_i are constants. Here we assumed that A_i^0 is proportional to the concentration of the i-th center. This implies that the A_i^0 parameter does not change from one isothermal decay to another, because we used the same crystal for the measurements. Using the above equation, we obtained a good fit with the parameters shown in table V. The dependence of A_i^0 with temperature

Insert Table V

show that the concentration of the center varies from one isothermal decay to another, which is in contradiction with the initial assumption that the concentrations does not change.

Thus we conclude that the kinetics of isothermal decay, as well as the irradiation growth, are very complex. A microscopic kinetic model analysis is in progress to describe the observed data.

In figure 9 we show the correlation between

Insert Figure 9

$\underline{k}//\underline{c}$-axis and $\underline{k} \perp \underline{c}$ - and (110)-axis bands at around 15,600 cm^{-1} for irradiation growth and thermal bleaching in colorless II sample. The correlation is linear, showing that we are dealing with a single polarized band.

In figure 10 we show the correlation between

Insert Figure 10

the 10,500 cm^{-1} and 15,600 cm^{-1} bands obtained for $\underline{k} \perp \underline{c}$- and (110)-axis for irradiation growth and thermal bleaching in colorless II sample. The correlation is linear, showing that we are dealing with two bands of the same center.

VI. DISCUSSION

The OA spectra of spodumene showed Fe bands only in green, yellow and colorless I samples (Fujii, 1981). As the colorless II sample showed larger Fe concentration than yellow and colorless I samples, we conclude that Fe doping is possible without inducing absorption in the visible. The Fe ion which does not show absorption in the visible, probably, is Fe^{3+} ion.

In green and yellow samples we see both Fe^{2+} electronic and $Fe^{2+} - Fe^{3+}$ charge transfer bands. Otherwise, in colorless I sample we see only the Fe^{2+} electronic band. This means that Fe^{3+} ions are found at, almost, two sites, one which does not allow absorption in the visible and the other which through interaction with Fe^{2+}, allow charge transfer band. In yellow sample the Fe^{2+} electronic band is bigger than in green and colorless I samples (Fujii, 1981; Fujii and Isotani, 1983), showing in this sample higher Fe^{2+} concentration. Otherwise, in green sample the bigger $Fe^{2+} - Fe^{3+}$ charge transfer bands shows higher Fe^{3+} concentration, which interacts with Fe^{2+}.

The Al^{3+} ion site, allow Fe^{2+} ion

substitution, with the charge stabilization, probably, being achieved through the substitution of Li^{+} ion by, for example, Ca^{2+} ion or by an interstitial alkali ion, like Na^{+}, neighbour to Fe^{2+} ion. The interstitial charge is expected to occupy a site between Li^{+} and Al^{3+} ion sites for better charge stabilization. So, for the sake of simplicity, we label the stabilization charge by X^{2+}-like ion, with X^{2+} site around Li^{+} ion site and along $Li^{+} - Al^{3+}$ axis.

The Fe^{2+} ion is, probably, at the plane LiAl formed by the Li^{+} and Al^{3+} ions (plane LiAl is parallel to the plane bc). Neighbour Fe^{2+} and X^{2+}-like ions at, for example, neighbour planes are at least 4.75 Å apart and are separated by SiSi plane (parallel to the plane bc), probably, giving a higher stabilization energy than any $X^{2+} - Fe^{2+}$ configuration at the LiAl plane.

The Li^{+} and Al^{3+} ion sites are neighbour along the c- and b-axis, respectively at distances around 2.6 Å and 3.3 Å. As both Li^{+} and Al^{3+} ion sites are surrounded by O^{2-} ions with three common O^{2-} ions, the best stabilization, with weaker structural distortion, probably, is achieved for smaller $X^{2-} - Fe^{2+}$ distance. So, we suggest for the structure of Fe^{2+} ion at the Al^{3+}

ion site, the formation of a X^{2+}:[Fe^{2+}] defect, with the X^{2+} - Fe^{2+} axis along the c-axis, and the brackets [ ] meaning the O^{2-} ions octahedral around the Fe^{2+} ion site. The d-d electronic transition of the Fe^{2+} ion in such distorted site give rise to the 6,100 and 9,000 cm^{-1} bands, consistent with that observed in other minerals (Burns, 1970, p. 87-105). A sketch of the X^{2+}:[Fe^{2+}] defect is shown in figure 11.

Insert Figure 11

The Fe bands in green, yellow and colorless I samples are not changed by irradiation nor by thermal treatments. This means that, probably, Fe is not found in Si^{4+} ion site and nor at interstitial sites. The substitution of Fe^{4+} ion in Si^{4+} ion site, must show a band at around 18,000 cm^{-1}, as observed in amethyst (Cohen, 1985). The Fe^{3+} ion substitution at Si^{4+} ion site, turns this site a hole trap, which under irradiation induces the formation of Fe^{4+} ion through the reaction $Fe^{3+} + h^{+} \rightarrow Fe^{4+}$, thus inducing the appearing of a band at around 18,000 cm^{-1}. The Fe^{3+} ion interstitial under irradiation turns Fe^{2+} ion by capture of an electron,

as shown for amethyst (Cohen, 1985). The interstitial Fe^{2+} ion show an OA band at around 12,000 cm^{-1}. Both 18,000 and 12,000 cm^{-1} were not observed in green, yellow and colorless I natural samples.

On the other hand, the 12,000 cm^{-1} band observed after irradiation in the polarized spectra of the colorless II sample, indicates the presence of interstitial Fe impurity and the reduction of interstitial Fe^{3+} ion into Fe^{2+} ion.

The site allowed for Fe^{3+} ion which does not allow OA electronic transition is, probably, at the Al^{3+} ion site (see figure 12). Irradiation and thermal treatments

Insert Figure 12

does not change Fe^{3+} ionization state, because the substitution is without change in the charge. This agrees with EPR measurements (Gait and Michoulier, 1973) which showed Fe^{3+} ion at Al^{3+} ion site. This Fe^{3+} ion, also, is not expected to show absorbance in the visible. Being a half-filled d-shell, the octahedral environment cannot allow Jahn-Teller distortion. Without the mixing of atomic orbitals promoted by the distortions, no change

in the d-orbitals parities are expected and so the d-d transition probabilities are negligible.

The Fe^{3+} ion which allow $Fe^{2+} - Fe^{3+}$ charge transfer bands must be near to Fe^{2+} ion. Because Fe^{3+} is substitutional to $A\ell^{3+}$, does not need charge stabilization, but Fe^{2+} needs. So, we suggest the Fe^{3+} ion is near to an $X^{2+}:[Fe^{2+}]$ defect. Two configurations are possible: (i) $[Fe^{3+}]$ group neighbour to X^{2+} with the $X^{2+} - Fe^{3+}$ axis along the b-axis, and with $Fe^{3+} - Fe^{2+}$ axis being around 52^{o} from the c-axis; (ii) $[Fe^{3+}]$ group neighbour to the Li^{+} ion along the b-axis, with $Li^{+} - Fe^{3+}$ axis perpendicular to the c-axis, and with $Fe^{3+} - Fe^{2+}$ axis being around 128^{o} from the c-axis. The Fe^{2+} and Fe^{3+} ions, in both cases, have three common O^{2-} ions, which makes possible the coupling between these ions through oxygen super-exchange interaction (Hippel, 1959, p. 265). The concentration of these defects depends on both $X^{2+}:[Fe^{2+}]$ defects as well as $[Fe^{3+}]$ group concentrations. Thus it is possible a case with bigger Fe^{2+} bands than the $Fe^{2+} - Fe^{3+}$ charge transfer band, like in the yellow sample, while charge transfer band is bigger in the green sample. The substitution of Fe^{3+} ion at the $A\ell^{3+}$ site increases the metal-oxygen covalent interaction, because

the electronegativity of Fe is bigger than of Aℓ. This turn $[Fe^{3+}]$ a shallow electron trap. The positive character of $[Fe^{3+}]$ makes the stabilization energy of the i-type configuration weaker than of the ii-type configuration. So, we assume here that the B-type Fe^{3+} defect is of ii-type configuration, as shown in figure 13.

Insert Figure 13

The $[Fe^{2+}]$ stabilized by a neighbour X^{2-}, have one electron excess. Thus $[Fe^{2+}]$ is able to capture one hole center in the oxygen ion around Fe^{2+}. The hole center, probably is localized around the three oxygen ions at opposite site from that of X^{2+}. Due to this delocalization, the hole will couple with the Fe-O vibrations. We estimate the EPR line width, ΔH, of the hole assuming the following assumptions: (a) each oxygen vibration promote spin relaxation; (b) the Fe-O vibrations are at about $\bar{\nu} = 500\ cm^{-1}$ (Nakamoto, 1963; Ross, 1972); (c) the uncertainty relation $\Delta E \Delta\tau \sim h$, where $\Delta E = g\ \Delta H$ and $\Delta\tau \sim 1/c\bar{\nu}$, can be applied. The value obtained is 3×10^{5} gauss, showing a big spin-vibration line broadening, which is beyond the usual range of measurements.

The X^{2+} is an electron trap, due to the excess of a +1e charge. An electron can be trapped at this center. Now, as $[Fe^{2+}]$ have an electron process, we expect an exchange interaction between the X^{2+} trapped electron and the net $[Fe^{2+}]$ electron excess, forming a H_2 like bond. This result is a deep electron trap and an equivalent spin of $s = 0$ for the trapped electron. Also, the partial decrease in the electron charge density at Fe^{2+} ion, due to the formation of a H_2 like bond, decreases the d-d transition probability.

Irradiation produce electrons and holes which can be trapped at the X^{2+} ions (deep electrons) of $X^{2+} : [Fe^{2+}]$ defect, at $[Fe^{3+}]$ (shallow electrons) and at $[Fe^{2+}]$ (holes) of $X^{2+} : [Fe^{2+}]$. On heating the trapped electrons are released and recombine with the holes trapped at $[Fe^{2+}]$. The excess of energy will be transferred to the Fe^{2+} ions. The lowest transition energy in Fe^{2+} is of around 6,000 cm^{-1} and the highest phonon energy is around 600 cm^{-1} (Imbush, 1978, p. 65). Therefore if non-radiative transition occurs across this 6,000 cm^{-1} gap, it involves the creation of around 10 phonons. As the order of perturbation theory needed is not so high, non-radiative decay can occur, and so

luminescence is not expected to be easily seen.

The Mn impurity in spoudmene is expected to be in $A\ell^{3+}$ ion site as Mn^{3+} ion. As the d-d transition is forbidden because d orbitals have the same parity, and even for small orbital mixing giving a small transition probability, the small concentration of Mn, makes the observation through OA spectra of Mn d-d transition very difficult.

The effective charges on Li^{+}, $A\ell^{3+}$, Si^{4+} and O^{2-} ions in spodumene was shown to be, respectively, +0.7e, +2.4e, +2.4e, ~ -1.3e (Sasaki et al., 1980). This show mixing between the atomic orbitals of positive and negative ions. The $A\ell^{3+}$ ion, with full filled d-shell, show about 20% less positive charge due to interaction with oxygen ions. On the other hand the half filled d-shell Mn^{2+} ion in Mn_2SiO_4 show an effective charge of +1.21e, showing a 40% less positive charge due to interaction with oxygen ions. Higher interaction metal-oxygen is expected for Mn^{3+} and the six octahedrally disposed oxygens. The substitution of Mn^{3+} at the $A\ell^{3+}$ site, increases the metal-oxygen interaction, turning the oxygen ion orbital less filled as related to the oxygen ions surrounding $A\ell^{3+}$ ions. So, the $[Mn^{3+}]$ group is a

shallow electron trap.

The EPR spectra of spodumene showed the presence of Mn^{2+} (Holuj and Manoogian, 1968), at the $A\ell^{3+}$ ion-site. The charge stabilization can be achieved through a X^{2+} neighbour to $[Mn^{2+}]$ forming a $X^{2+}:[Mn^{2+}]$ defect. This defect, as in $X^{2+}:[Fe^{2+}]$ defect, have X^{2+}-Mn^{2+} axis along the c-axis. A trapped hole in the oxygens fartest from X^{2+}-like ion, as in $X^{2+}:[Fe^{2+}]$ will not be seen in the EPR spectra. The recombination of the hole with an electron in the oxygens around Mn^{2+}, promote through energy transfer Mn^{2+} to excited states. The excess of energy is dissipated through phonons to the first excited state $^4T_{1g}$ and so to the ground state through $^4T_{1g} \rightarrow {}^6A_{1g}$ luminescence (Marfunin, 1979, p. 195-196). The observation of an orange luminescence (Fujii, 1981) in lilac spodumene agrees with the present consideration. The configuration of this defect is similar to the $X^{2+}:[Fe^{2+}]$ defect shown in figure 11.

Let us now consider the assignment for the polarized spectra at around 10,500, 15,600 and 21,000 cm^{-1}, which we show to arise from a single center. The Mn^{2+} EPR spectra does not showed any change under irradiation (Ito, 1980). So, these bands must be assigned to Mn^{3+}

or Mn^{4+}. Ito (1980) assigned these bands to Mn^{3+} through a crystal field analysis. The electronegativity of Mn(1.7) is bigger than of Aℓ(1.6). Thus the substitution of Mn^{3+} at $A\ell^{3+}$ site, increases the metal-oxygen covalent interaction. This induces a small decrease in the electron charge density at the O^{2-} ions. So, $[Mn^{3+}]$ group is able to receive additional charge density, turning a shallow electron trap. The center of the bands here referred was produced by irradiation. Thus, we propose that the precursor defect at $A\ell^{3+}$ site, Mn^{4+}, is reduced into Mn^{3+} by trapping an electron. Otherwise, we drop the possibility of oxidation of Mn^{3+} into Mn^{4+} because $[Mn^{3+}]$ is a shallow electron trap.

The precursor defect $[Mn^{4+}]$ introduces a +1e charge excess at $A\ell^{3+}$ site. This defect can be stabilized by: (i) a neighbour Li^+ vacancy; (ii) $A\ell^{3+}$ substitution by an +2e charged ion, for example, Ca^{2+}, Fe^{2+} or Mn^{2+}, which we label as Z^{2+}. These configurations results in two possible symmetries for the defect. As the Mn^{4+} spectra was not seen, the local symmetry of the defect must be analysed through the polarized spectra of Mn^{3+}.

The first configuration i shown in figure

14, with a Li^+ vacancy have the weaker stabilization

Insert Figure 14

energy if the vacancy is at the first neighbour site along the c-axis. In this configuration, the Li^+ vacancy, acting as an -1e defect, repel three oxygen ions into Mn^{4+} direction. Also, the Mn^{4+} ion attracts these oxygen ions like a +1e charge. The resultant distortion in the oxygen octahedra around Mn^{4+} ion is expected to be high. This high distortion mix the atomic orbital of Mn^{4+} changing its parity. Thus, the transition probability will be no longer equal to zero, as for octahedral symmetry. In this case, a spin-forbidden absorption band at around 16,000 cm^{-1} is expected as seen in K_2MnF_6 (Jorgensen, 1958). However, as the Mn concentration is about 200 to 600 times weaker than in K_2MnF_6, this band should be hardly observed.

The Li^+ vacancy along the c-axis induces a dipole moment along this axis. This will give zero transition probability for $\underline{E}$ perpendicular to the c-axis. In the spectra of spodumene we found that the 18,600 cm^{-1} band show an almost complete extinction for

$\underline{E}$ around 60^o from the c-axis in the (110)-plane. As polarization follow Malus' cosine law, we conclude that complete extinction is possible for $\underline{E}$ at 90^o from the c-axis in agreement with the Li^+ vacancy neighbour to Mn^{4+} ion along the c-axis. For Fe rich samples, probably, high amounts of Fe^{2+} are stabilized through interstitial Na^+ ions. The resultant high concentrations of alkaline ions in the network, probably, prevents the formation of Li^+ vacant defects, explaining the absence of 18,600 cm^{-1} band in Fe rich samples. The higher crystal field parameters found for Mn^{3+} in b-site, is also consistent with the high distortion of the oxygen octahedra.

The second configuration ii, with a Z^{2+} ion, have the weaker stabilization energy if the ion is at the first neighbour Aℓ, as shown in figure 15. The

Insert Figure 15

$Mn^{4+} - Z^{2+}$ distance is about 4.2 Å. The relative decrease of the local charge at $Aℓ^{3+}$ site is about 1/3 of the Li^+ vacancy, and only one oxygen ion is repelled. This kind of stabilization introduces only a small distortion in

the octahedral crystal field symmetry. The d-d transition probability being small in Mn^{4+} and being the Mn concentration about 400 times smaller than in K_2MnF_6, no 16,000 cm^{-1} band is expected. Thus we conclude that the best stabilization configuration model for Mn^{4+} is that of Z^{2+} ion substitution at the first neighbour $A\ell^{3+}$ site.

The reduction of Mn^{4+} into Mn^{3+} through the trapping of an electron charge, is followed by a big change in the transition probability. The net negative charge at the Z^{2+} site is distributed along the O^{2-} ions, perhaps, increasing the net value -1.3e. The electron trapped in Mn^{3+} is also an excess of negative charge, because the charge distribution around Mn^{4+} turns this site neutral for +4e ion. So, the excess of negative charge density is found between Mn^{3+} site and the oxygen ion common to Mn^{3+} and Z^{2+}. This give rise to a H_2 like bond extending for all oxygens around Z^{2+} ion, and the parity of the Mn^{3+} d-orbitals are no longer preserved. The covalent character of this interaction will give a big transition probability giving rise to strong absorption bands. The analysis of the polarized spectra, due to the complexity of the wave functions and dipole moment tensor, is beyond the scope of the present work.

ACKNOWLEDGMENTS

The present work was supported partially by grants of CAPES-PICD, FAPESP, CNPq and FINEP.

REFERENCES

Bevington, P.R. (1969) Data reduction and error analysis for the physical sciences. McGRaw-Hill Book Co, New York.

Blak, A.R., Isotani, S. and Watanabe, S. (1982) Optical absorption and electron spin resonance in blue and green natural beryl. Physical Chemistry of Minerals, 8, 161-166.

Burns, R.G. (1970) Mineralogical applications of crystal field theory. Cambridge at the University Press,

Claffy, E.W. (1953) Composition, tenebrescence and luminescence of spodumene minerals. American Mineralogist, 38, 919-931.

Cohen, A.J. (1985) Amethyst color in quartz, the result of radiation protection involving iron. American Mineralogist, 70, 1180-1185.

Cohen, A.J. and Janezic, G.G. (1983) The crystal-field spectra of the $3d^3$ ions, Cr^{3+} and Mn^{4+} in green spodumenes, the significance of trace elements in solving petrogenetic problems & controversies. Theophrastus Pulications S.A., Athens, p. 899-904.

Dana, J.M. and Hurlbut, Jr., C.S. (1978) Dana's manual of mineralogy. Livros Técnicos e Científicos, Rio de Janeiro.

Deer, W.A., Howie, R.A. and Zussman, J. (1966) Rock forming minerals, vol. 2. Logan, London.

Fujii, A.T. (1981) Comparative study of several varieties of spodumene by optical and electron resonance spectroscopy. Ms. Thesis, University of São Paulo, São Paulo, Brazil.

Fujii, A.T. and Isotani, S. (1982) Thermal equilibrium measurements in spodumene crystal. Semina, 3, 269-272.

Gait, J.M. and Michoulier, J. (1973) Electron paramagnetic resonance of Fe^{3+} in diopside and spodumene. Journal of Chemical Physics, 59, 488-494.

Hassan, F. and Labib, M. (1978) Induced colour centers in α-spodumene called kunzite. Neues Jahrbuch für Mineralogie Abhandlungen, 134, 104-115.

Hippel, A.R. von (1959) Molecular Science and Molecular Engineering. The Technology Press of Massachussets Institute of Technology. John Wiley and Sons, Inc., New York.

Holuj, F. (1968) EPR of Mn in spodumene. I. Natural crystals. Canadian Journal of Physics, 46, 287-302.

Holuj, F. and Manoogian, A. (1968) EPR of Mn in spodumene. II. Heated crystals. Canadian Journal of Physics, 46, 303-306.

Imbusch, G.F. (1978) Inorganic luminescence. In Luminescence Spectroscopy, Ed. Lumb, M.D.. Academic Press, London, New York, San Francisco.

Ito, A.S. (1980) Study of radiation damage and heat treatment in spodumene. Ph.D. Thesis, University of São Paulo, São Paulo, Brazil.

Jorgensen, C.K. (1958) Acta Chemica Scandinava, 12, 1539 (not seen; extracted from Cohen and Janezic, 1983).

Leckebusch, R., Recker, K. and Triché, C. (1974) Notes des membres et correspondants et notes presentées ou transmises par leurs soirs. Comptes Rendus de l'Academie des Sciences de Paris, 278, 1541-1544.

Levy, P.W., Mattern, P.L., Lengweiler, K. and Bishay, A. M. (1974) Studies on nonmetals during irradiation: V, growth and decay of color centers in barium aluminoborate glasses containing cerium. Journal of American Ceramic Society, 57, 176-181.

Manoogian, A., Holuj, F. and Carwell, J.W. (1965) The electron spin resonance of Fe^{3+} in single crystals of spodumene. Canadian Journal of Physics, 43, 2262-2275.

Marfunin, A.S. (1979) Spectroscopy, luminescence and radiation centers in minerals. Springer-Verlag, Berlin, Heidelberg, New York.

Nakamoto, K. (1963) Infrared spectra of inorganic and coordination compounds. John Wiley and Sons, Inc., New York.

Ross, S.D. (1972) Inorganic Infrared and Raman spectra. McGraw-Hill Book Co, New York.

Sasaki, S., Fujino, K., Takeuchi, Y. and Sadanaga, R. (1980) On the estimation of atomic charges by the X-ray method for some oxides and silicates. Acta Crystallographica, A36, 904-915.

Schmitz, B. and Lehmann, G. (1975) Colour centers of manganese in natural spodumene $LiAlSi_2O_6$. Bunsengesellschaft fuer Physikalische Chemie. Berichte, 79, 1044-1049.

Takeuchi, N., Inabe, K. and Nanto, H. (1975) Note on the isothermal decay method for determining trap depth from glow curves. Journal of Material Sciences, 10, 159.

White, W.B. and Keester, K.L. (1966) Optical absorption spectra of iron in the rock-forming silicates. American Mineralogist, 51, 774-791.

TABLE I - Concentration of Fe, Cr and Mn in spodumene.

Sample	[Fe] (ppm)	[Mn] (ppm)	[Cr] (ppm)	[Fe]/[Mn]
Lilac A	160 ± 10	460 ± 10	90 ± 20	0.35
Lilac B	140 ± 10	240 ± 10	90 ± 20	1.71
Colorless I	190 ± 10	180 ± 10	100 ± 20	1.06
Colorless II	390 ± 10	110 ± 10	90 ± 20	3.55
Yellow	320 ± 10	200 ± 10	90 ± 20	1.6
Green	1720 ± 10	500 ± 10	190 ± 20	3.44

TABLE II - Optical absorption band-maxima in cm^{-1}.

Lilac A	Colorless I	Colorless II	Colorless II (irradiated)	Green	Yellow	Assignment from Ito (1980)	Present assignment
no	no	6,100 (w)		6,100 (m)	6,100 (s)		Fe^{2+} in distorted octahedral site
no	no	9,300 (w)		9,100 (m)	8,900 (s)		
11,000 (vw)	no	11,000 (b)	10,500 (s)	no	no	Mn^{3+}(a)	
15,600 (b)	no	no	15,600 (s)	no	no		
no	no	no	22,000 (w)	no	no		
no	no	11,500 (vw)		no	no		
no	no	no		16,000 (s)	16,000 (m)		$Fe^{2+} - Fe^{3+}$ charge transfer
no	no	no		19,500	19,500		
18,600 (s)	no	18,600 (b)		no	no	Mn^{3+}(b)	electron trapped at X^{2+} ion; X^{2+} : $[Mn^{2+}]$
22,800 (sh)	22,800 (sh)	22,800 (vw)		22,800 (w)	22,800 (m)		Mn^{2+} in octahedral site
23,000 (sh)	23,000 (sh)	23,000 (vw)		23,000 (w)	23,000 (m)		
25,200 (sh)	25,200 (sh)	25,200 (vw)		25,200 (vw)	25,000 (sh)		
25,900 (sh)	25,900 (sh)	25,900 (vw)		25,900 (vw)	25,900 (sh)		
24,000	25,600	30,300		29,000	26,000		Band-edge (OD=0.5)

sh = shoulder; b = broad; vw = very weak; w = weak; m = medium; s = strong.

TABLE III - Parameter fit for three gaussians.

		1	2	3
ν_{0_i} (10^3 cm^{-1})	$\perp c$	9,15 ± 0,06	11,03 ± 0,06	15,08 ± 0,01
	$//c$	9,2 ± 0,1	10,5 ± 0,1	15,3 ± 0,3
A_{0_i}	$\perp c$	0,29 ± 0,02	0,24 ± 0,02	0,50 ± 0,01
	$//c$	0,028 ± 0,002	0,016 ± 0,06	0,657 ± 0,003
σ (10^{-8} cm^{-1})	$\perp c$	30 ± 1	336 ± 1	23 ± 1
	$//c$	77 ± 5	285 ± 9	26 ± 1

TABLE IV - Parameters a and b of $A(t) = A_0 (1 + at)^{b}$.

T (^{o}C)	a	b	n
120	0.0145	- 0.331	4.02
136	0.0234	- 0.508	2.97
154	0.0864	- 0.385	3.59
163	0.315	- 0.463	3.15

TABLE V - Parameters A_{0_i} and b_i for three first order decays.

T (^{o}C)	A_{0_1}	A_{0_2}	A_{0_3}	b_1	b_2	b_3
120	0.156	0.323	0.517	0.076	0.0037	0.00027
136	0.255	0.557	0.231	0.102	0.0041	0.00028
154	0.345	0.464	0.244	0.096	0.0084	0.00035
163	0.492	0.340	0.009	0.176	0.0116	0.00038

FIGURE CAPTIONS

Figure 1 - Polarized optical absorption spectra of colorless II spodumene sample.

Figure 2 - Growth of the 15,600 cm^{-1} band with the irradiation dose.

Figure 3 - Fit of the spectrum for $\underline{k} // \underline{c}$-axis.

Figure 4 - Fit of the spectrum for $\underline{k} \perp \underline{c}$-axis.

Figure 5 - Change of the spectra with $\underline{k}$ along the plane $\perp$ (110)-axis.

Figure 6 - Polarized optical absorption spectra in the plane $\perp$ $\underline{c}$-axis.

Figure 7 - Polarized optical absorption spectra in the plane $\underline{k} //$ (110)-axis.

Figure 8 - Thermal decay of the 15,600 cm^{-1} band.

Figure 9 - Correlation between the irradiation growth and thermal bleaching with the 15,600 cm^{-1} band for $\underline{k} // \underline{c}$-axis and $\underline{k} \perp \underline{c}$ and (110)-axis.

Figure 10 - Correlation between the irradiation growth and thermal bleaching of 10,500 cm^{-1} and 15,600 cm^{-1} bands.

Figure 11 - Sketch of $X^{2+} : [Fe^{2+}]$ defect.

Figure 12 - Sketch of Fe^{3+} ion site.

Figure 13 - Sketch of the $X^{2+} : [Fe^{2+}] : [Fe^{3+}]$ defect.

Figure 14 - Sketch of the Li^{+} vacancy stabilized $[Mn^{4+}]$ defect.

Figure 15 - Sketch of the $Z^{2+} : [Mn^{4+}]$ defect.

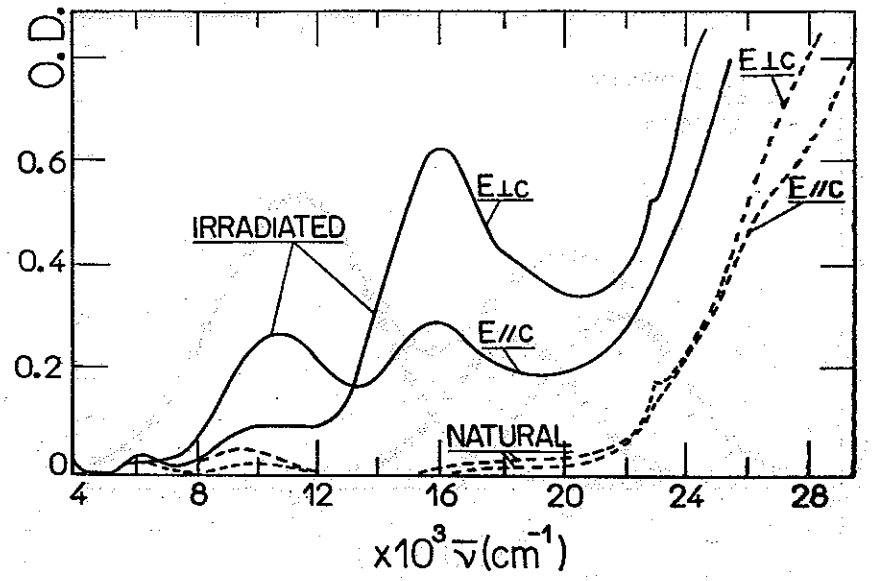

Figure 1 - Polarized optical absorption spectra of colorless II spodumene sample.

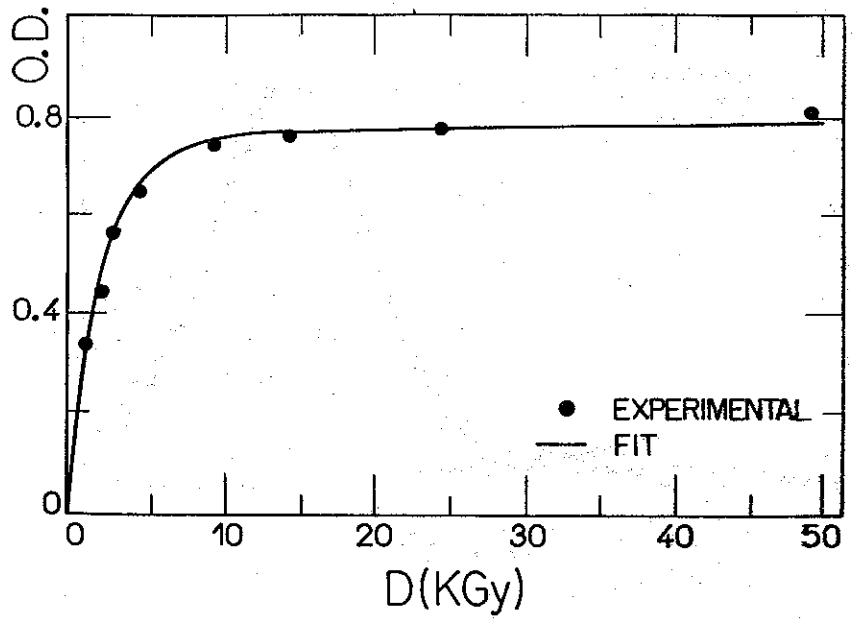

Figure 2 - Growth of the 15,600 cm^{-1} band with the irradiation dose.

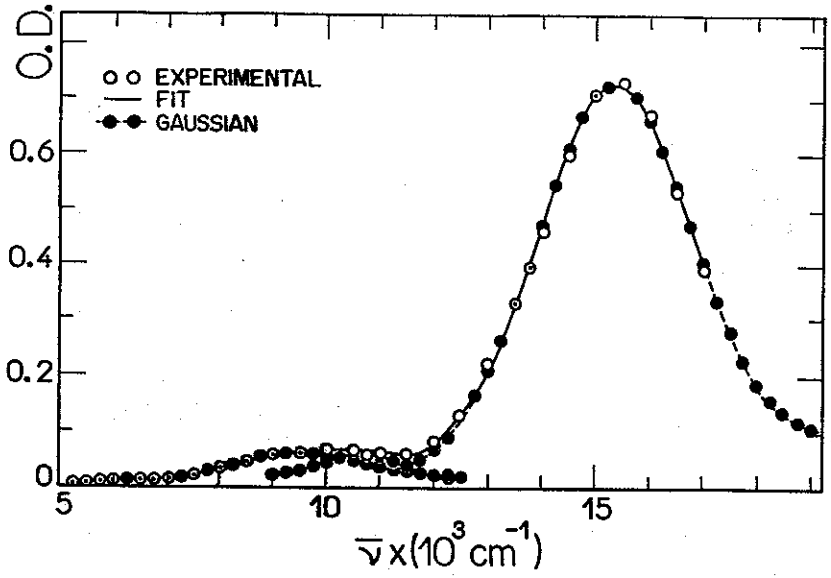

Figure 3 - Fit of the spectrum for $\underline{k}//\underline{c}$-axis.

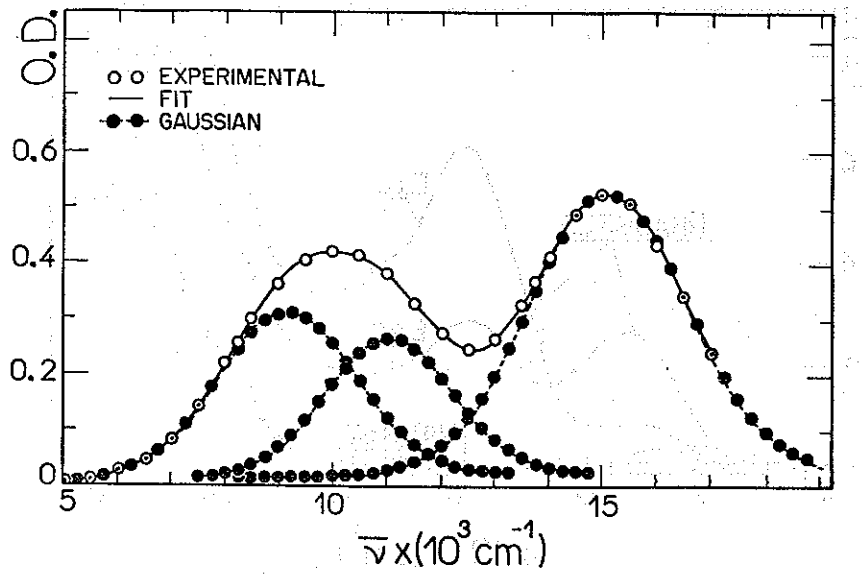

Figure 4 - Fit of the spectrum for $\underline{k} \perp \underline{c}$-axis.

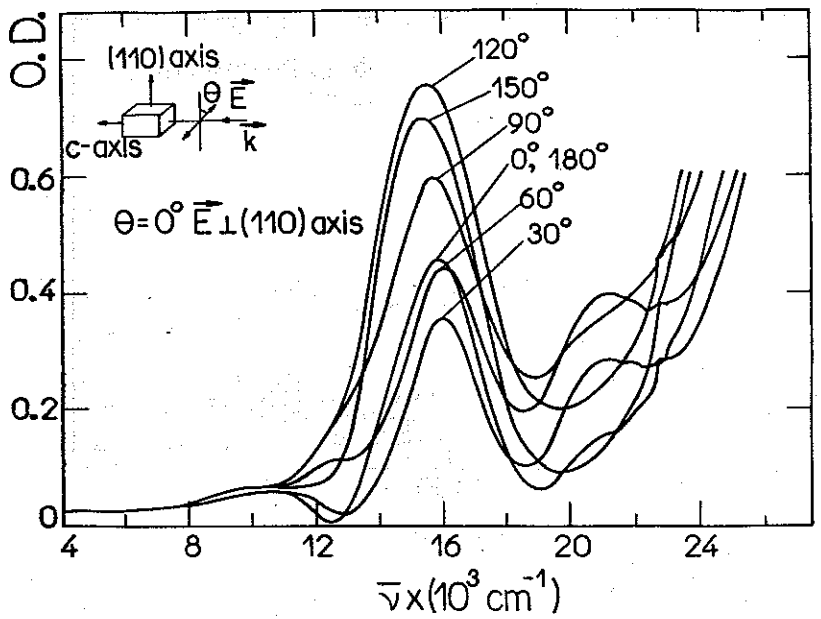

Figure 5 - Change of the spectra with $\underline{k}$ along the plane $\perp$ (110)-axis.

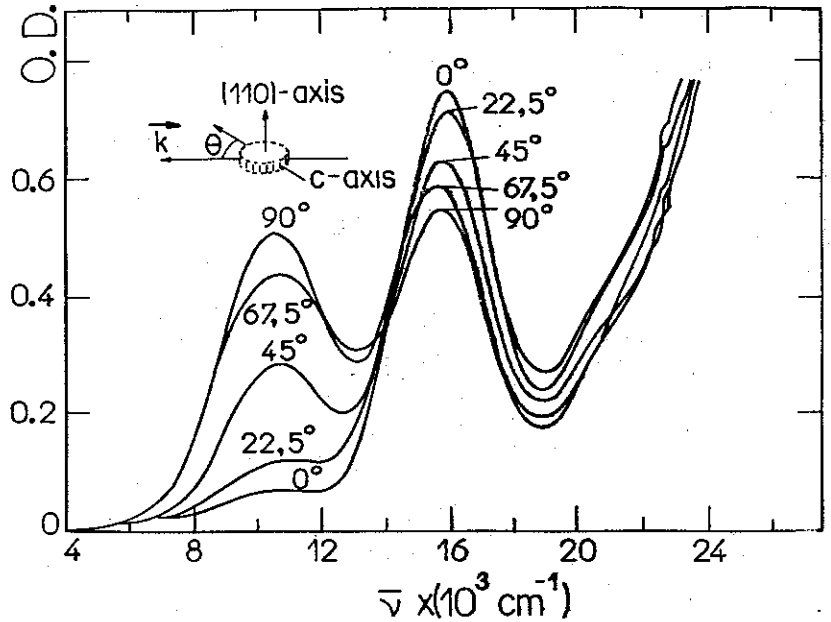

Figure 6 - Polarized optical absorption spectra in the plane $\perp$ $\underline{c}$-axis.

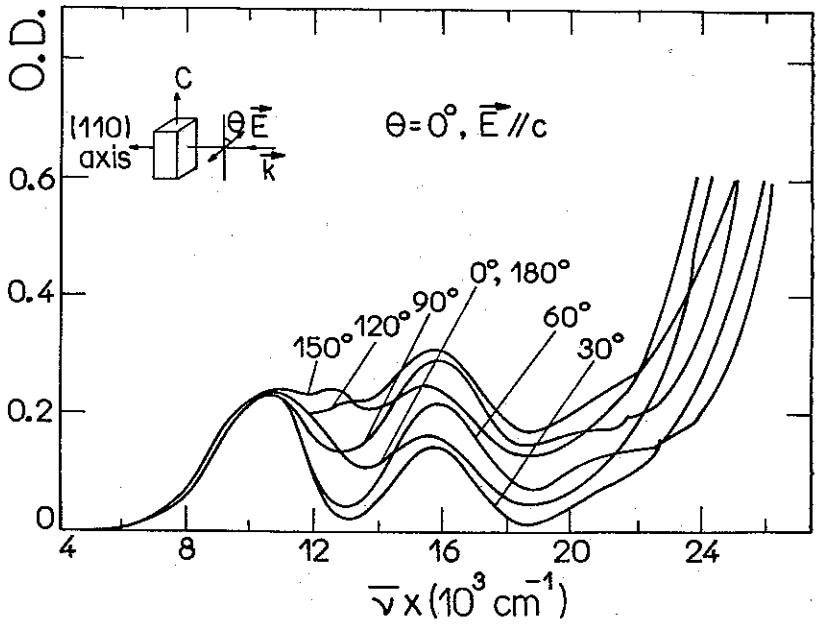

Figure 7 - Polarized optical absorption spectra in the plane k//(110)-axis.

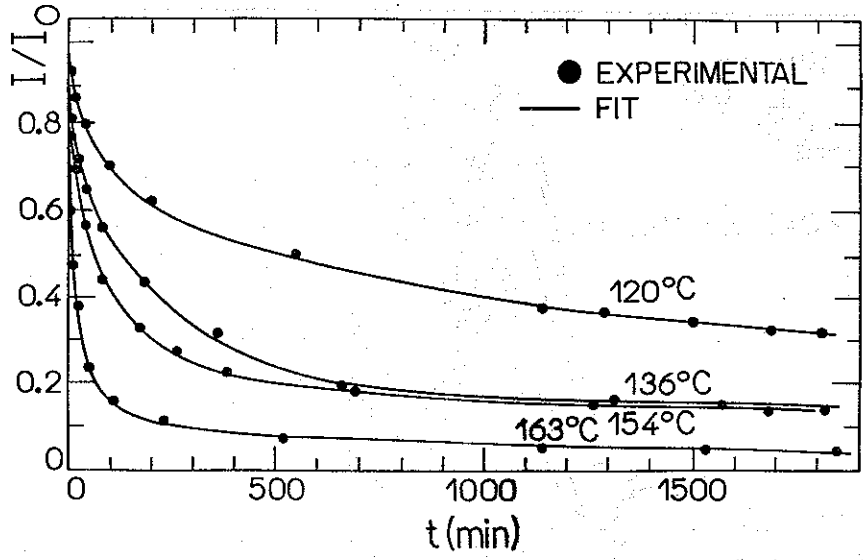

Figure 8 - Thermal decay of the 15,600 cm^{-1} band.

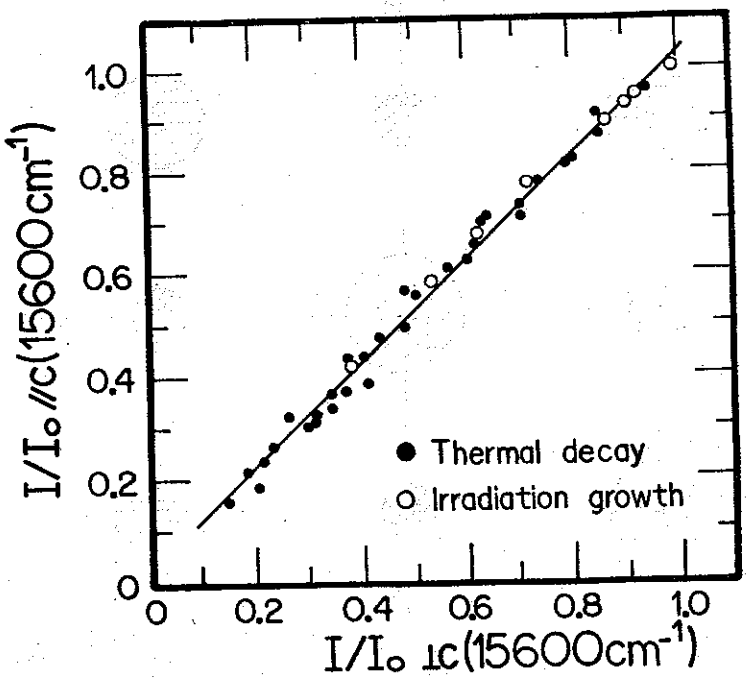

Figure 9 - Correlation between the irradiation growth and thermal bleaching with the 15,600 cm^{-1} band for $\underline{k}//\underline{c}$-axis and $\underline{k} \perp \underline{c}$ and (110)-axis.

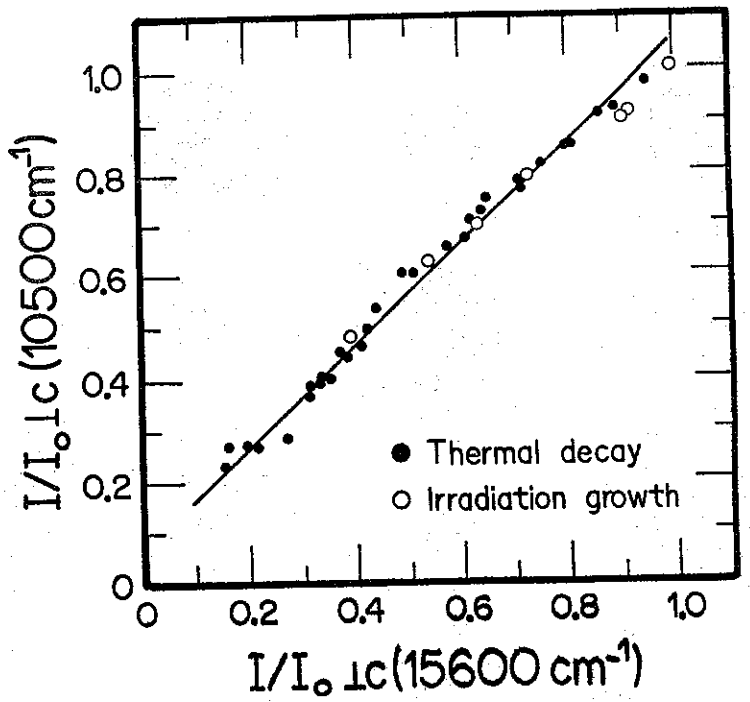

Figure 10 - Correlation between the irradiation growth and thermal bleaching of 10,500 cm^{-1} and 15,600 cm^{-1} bands.

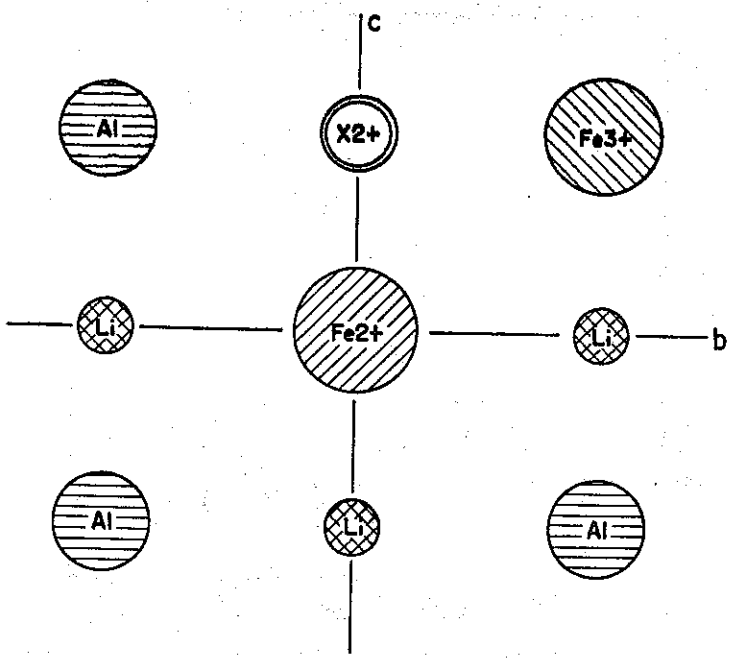

Figure 11 - Sketch of $X^{2+}:[Fe^{2+}]$ defect.

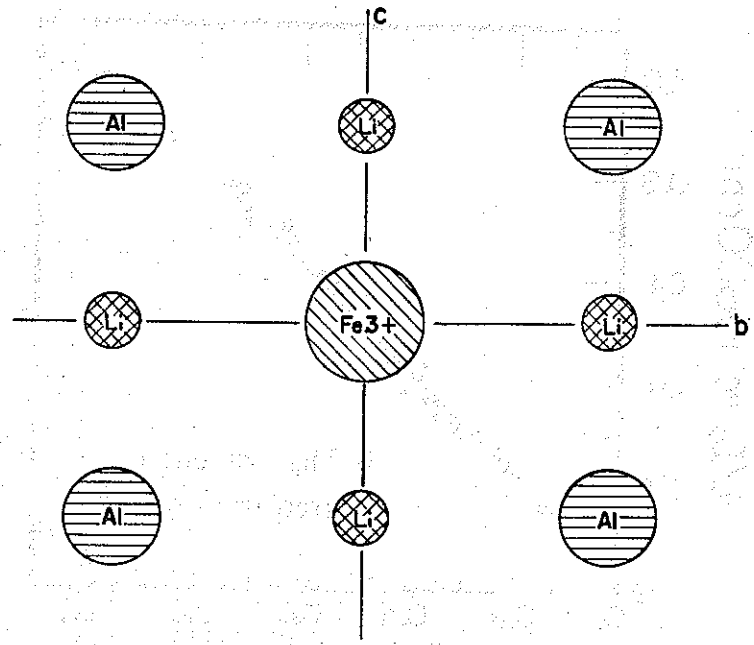

Figure 12 - Sketch of Fe^{3+} ion site.

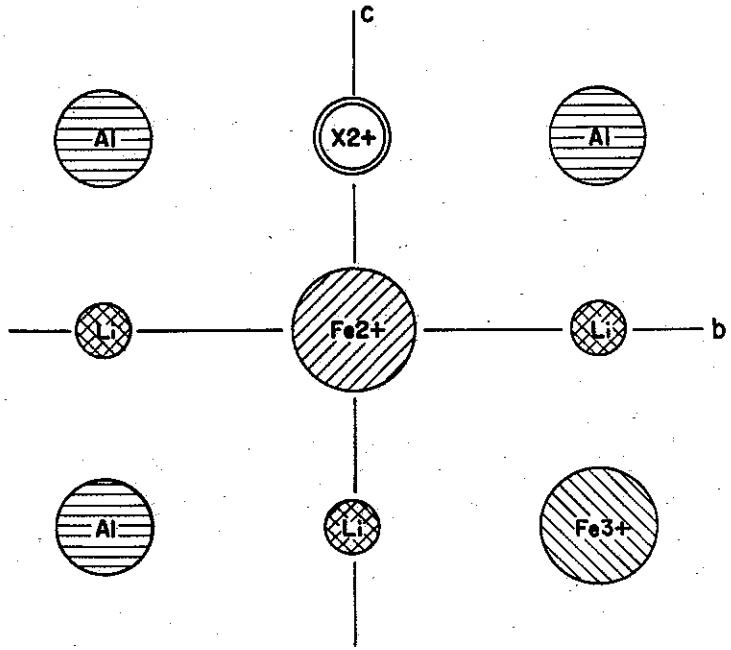

Figure 13 - Sketch of the X^{2+} : $[Fe^{2+}]$: $[Fe^{3+}]$ defect.

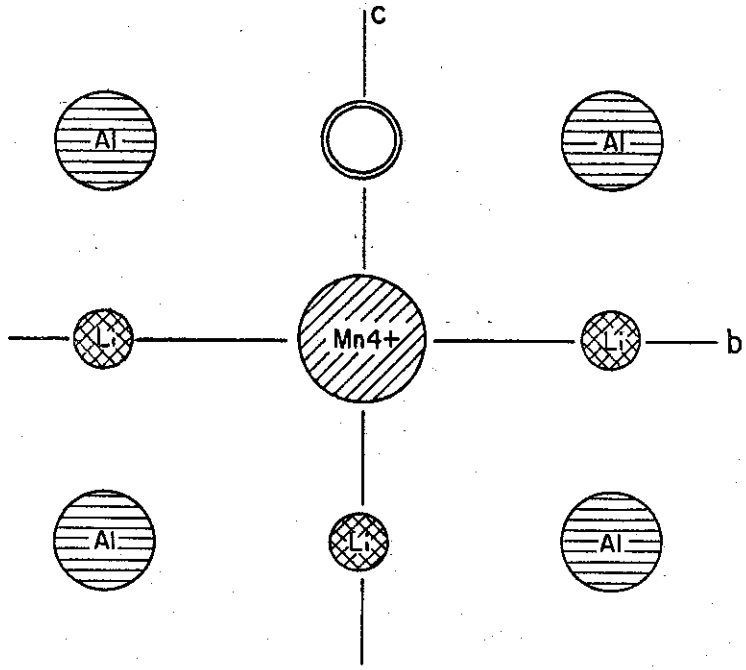

Figure 14 - Sketch of the Li^{+} vacancy stabilized $[Mn^{4+}]$ defect.

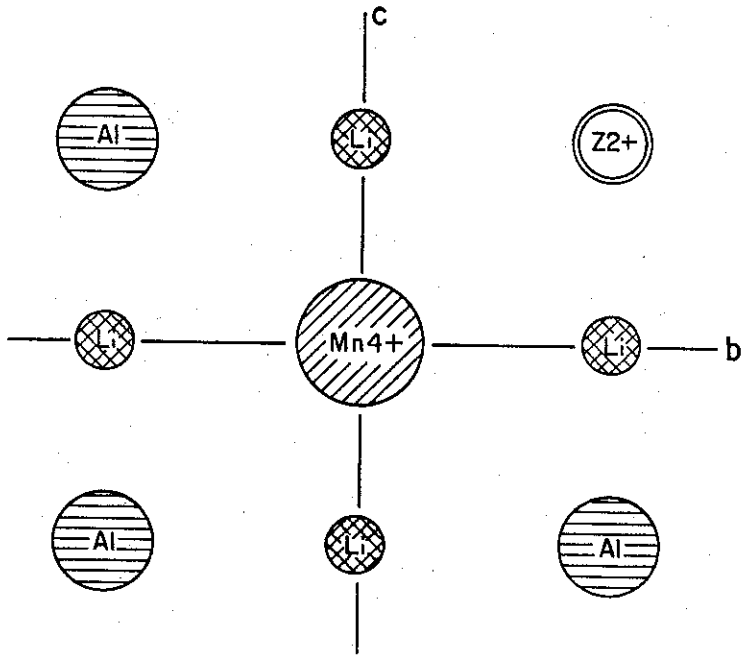

Figure 15 - Sketch of the $Z^{2+}:[Mn^{4+}]$ defect.